Magnetic Mirror Structure for Testing Shell-type Quadrupole Coils

N. Andreev, E. Barzi, R. Bossert, G. Chlachidze, V. S. Kashikhin, V. V. Kashikhin, M. J. Lamm, F. Nobrega, I. Novitski, M. Tartaglia, D. Turrioni, R. Yamada, A. V. Zlobin

***Abstract*—This paper presents magnetic and mechanical designs and analyses of the quadrupole mirror structure to test single shell-type quadrupole coils. Several quadrupole coils made of different Nb_3Sn strands, cable insulation and pole materials were tested using this structure at 4.5 and 1.9 K. The coils were instrumented with voltage taps, spot heaters, temperature sensors and strain gauges to study their mechanical and thermal properties and quench performance. The results of the quadrupole mirror model assembly and test are reported and discussed.**

***Index Terms*—Quadrupole coil, magnetic mirror, magnet test.**

I. INTRODUCTION

FERMILAB is involved in the development of a new generation of accelerator magnets with operation fields in accelerators above 10 T and increased operation margins based on Nb_3Sn superconductor. The development and implementation of this new technology involves fabrication and test of a series of magnet models, coils and other components with various design and processing features, and structural materials. To provide an efficient way to test and optimize Nb_3Sn quadrupole coils a quadrupole magnetic mirror was developed at Fermilab based on the positive experience gained during Nb_3Sn dipole coil testing with a dipole mirror structure [1, 2]. This approach allowed testing individual coils at the operating conditions similar to that of a real magnet, thus reducing the turnaround time of coil fabrication and evaluation, as well as material and labor costs. Long dipole mirror magnets were also successfully used for the Nb_3Sn coil technology scale-up [3, 4]. Implementation of the mirror configuration for a quadrupole magnet offers even greater benefits due to the larger number of coils in quadrupoles with respect to dipole magnets.

This paper describes the magnetic and mechanical design of a quadrupole mirror structure for testing single shell-type superconducting quadrupole coils with the aperture from 90 to 120 mm. The concept was experimentally verified by testing LARP 90-mm Nb_3Sn quadrupole coils [13] in the developed mirror structure in the temperature range of 1.9-4.5 K. The fabrication experience and test results of the quadrupole mirror models are reported and discussed.

Manuscript received 21 October 2009. This work supported by Fermi Research Alliance, LLC, under contract No. DE-AC02-07CH11359 with the U.S. Department of Energy.

Authors are with the Fermi National Accelerator Laboratory (Fermilab), P.O. Box 500, Batavia, IL 60510 USA (phone: 630-840-8192; fax: 630-840-3369; e-mail: zlobin@fnal.gov).

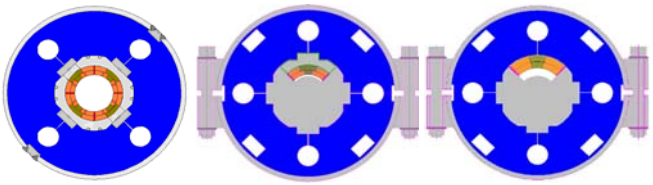

Fig. 1. TQC quadrupole cross-section with 4 collared coils inside the iron yoke and SS skin (a) and quadrupole mirror cross-sections with single 90-mm TQ coil (b) and 120-mm HQ coil (c) inside the iron yoke and bolted skin.

II. MAGNETIC AND MECHANICAL DESIGN AND ANALYSIS

The proposed quadrupole mirror design is based on the mechanical structure of LARP 90-mm quadrupole of the TQC series [6] shown in Fig. 1 (a). Three coils, stainless steel collar blocks and preload control spacers in the quadrupole structure were replaced by the magnetic mirror blocks and spacers as shown in Fig. 1 (b). This sub-assembly is installed in the standard TQC iron yoke and pre-compressed by a bolted stainless steel skin. To provide better matching of magnet transfer functions and Lorentz force distribution in the 90-mm quadrupole mirror and complete quadrupole models the space between the iron mirror and the coil inner surface was reduced to 5 mm [7]. The larger 120-mm HQ coil [8] could be accommodated in the same mirror structure by removing the iron spacer placed between the coil and iron yoke, and making the inner surface of corresponding iron yoke round.

Magnetic flux distribution at high current in the coil inside a TQM mirror with 90-mm coil (left) and a corresponding TQC quadrupole model (right) is shown in Fig. 2. The maximum field in cross-section in both quadrupoles and quadrupole mirrors is reached in the inner-layer pole turns. While in general both distributions look quite similar, some small differences can be noticed in the coil midplane turns. As can be seen later on, these differences reduce the azimuthal component of Lorentz force and eddy current losses in the midplane turns in the mirror configuration.

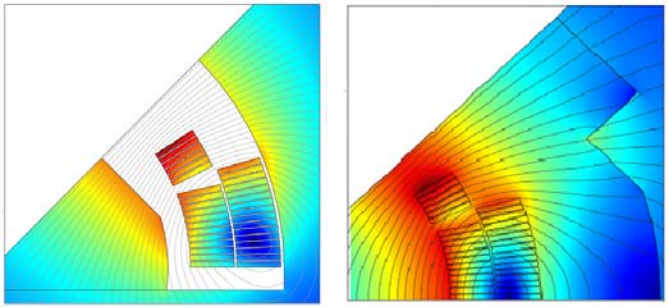

Fig. 2. TQM (left) and TQC (right) cross-sections with flux distribution at 14 and 12 kA respectively.

Table 1 Comparison of TQM/HQM mirrors and TQC/HQ quadrupole magnet parameters.

Parameter	Unit	90-mm		120-mm	
		TQM	TQC	HQM	HQ
Quench G @ 1.9K	T/m	n/a	254.5	n/a	219.8
Quench B_p @ 1.9K	T	13.84	13.66	15.11	15.29
Quench I @ 1.9K	kA	14.91	15.48	20.32	19.57
Inductance @ quench	mH/m	1.14	4.54	1.68	7.71
Stored energy @ quench	MJ/m	0.127	0.544	0.347	1.48

The iron yoke in TQM is extended over the coil ends, and the mirror block and the spacer between coil and yoke are of the same length as the iron yoke. For these reasons, the peak field point belongs to the coil end at the outer-layer pole turn. The ratio between the peak field in the end and in the straight section is not constant because of the large iron saturation varying from 0.99 at 4 kA to 1.06 at 16 kA. Depending on the length of the iron yoke, the HQM magnet may also have peak field point in the coil end that will be a subject of a separate analysis when the magnet details are finalized.

The generic short sample limits of the quadrupole mirror magnet was estimated based on the parameterization of critical current for Nb_3Sn superconductor [9] with the upper critical field B_{c2}=26 T, the critical temperature T_c=18 K and the reference critical current density J_c=3000 A/mm^2 at 12 T and 4.2 K. The Cu:nonCu ratio was 0.87. The quench parameters of mirror and quadrupole models are summarized in Table 1.

Lorentz forces in the TQM/HQM mirror and quadrupole models at quench current are shown in Table 2. The horizontal Lorentz force in the TQM/HQM mirrors is nearly the same as in the TQC/HQ quadrupole magnets, while the vertical force at high currents is ~30% lower. The azimuthal Lorentz force in TQM mirror at maximum quench current is a factor of 2.5-3 lower than in the quadrupole models due to the different field distribution in the midplane turns in the mirror. The azimuthal Lorentz force per the inner coil layer in HQM is nearly zero due to strong saturation of the magnetic mirror in the vicinity of the coil midplane, while the azimuthal force per the outer layer retains ~55 % of the original magnet value.

Stress distribution diagrams for the TQ and HQ coils in corresponding mirror configurations calculated using ANSYS at room temperature, after cooling down to 4.5 K and at the magnet current of 14 kA (TQM) and 17 kA (HQM) are shown in Figs. 3 and 4. As can be seen, the maximum coil pre-stress after cooling down of ~130 MPa allows keeping the TQ coil in TQM mirror under compression up to its ultimate short sample limit ~14 kA, whereas to keep HQ coil in HQM under compression up to ~17 kA (~85% of its short sample limit) the required coil cold pre-stress increases to ~150 MPa. Due to the larger azimuthal length in TQM the coil inner layer is unloaded earlier than the outer layer. In HQM the outer layer is unloaded earlier than the inner layer due to the larger azimuthal length.

Table 2 Lorentz forces in TQM/HQM mirror and quadrupole models at quench current (octant forces @ quench).

Parameter	Unit	90-mm		120-mm	
		TQM	TQC	HQM	HQ
F_x total	MN/m	1.67	1.67	3.33	3.38
F_y total	MN/m	-1.75	-2.56	-3.41	-5.03
F□ IL/OL	MN/m	0.36/0.70	1.15/1.78	0.13/1.76	2.63/3.15

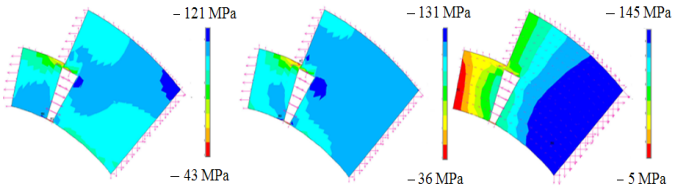

Fig. 3. Coil stress in TQM at 300 K after assembly, and after cooling down to 4.5 K at 0 and 14 kA.

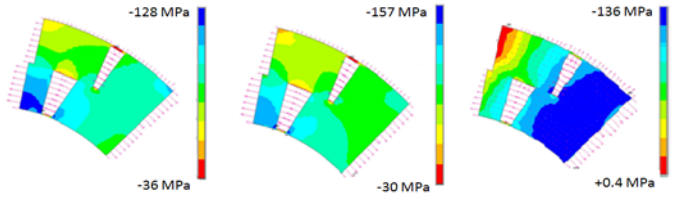

Figure 4. Stress distribution in the HQ coil in mirror configuration at 300 and 4.5 K at 0 and 17 kA.

III. TQM Mirror Model Assembly and Design Features

A. *Model Design Features*

Four quadrupole mirror models, TQM01, TQM02, TQM03a and TQM03b, were fabricated and tested in January-August 2009. The first two models, TQM01 and TQM02, used TQ coils previously tested in TQC quadrupoles [10]. The primary goal of these tests was to verify the quadrupole mirror design concept and assembly procedure, and compare coil quench performance in the quadrupole mirror with TQ models. The third mirror model TQM03 was assembled with a new TQ coil made of improved Nb_3Sn RRP strand of 108/127 design [11] and tested twice with two different coil pre-load levels. The cable for this coil was fabricated using Fermilab's cabling machine [12] and insulated with E-glass tape using standard cable insulating technique. The acceptable performance of this insulation for Nb_3Sn coils was confirmed previously by testing ten-stack samples [13] and 4-m long Nb_3Sn dipole coil [14].

The baseline TQ coil design is described in [5]. The coil specific features are summarized in Table 3.

B. *Assembly*

The mirror magnet assembly starts with installation of iron mirror blocks into the lower yoke placed inside the stainless steel (SS) skin. The coil, wrapped with multilayer ground insulation, is then placed onto the mirror and the iron spacers, upper yoke blocks (TQM) and/or the upper skin installed. The coil ground insulation consists of 4 layers of 75-125 μm Kapton. Thick G10 spacers are added in the coil midplanes to accommodate coil size variations and instrumentation (strip heaters, strain and temperature gauges, etc.).

Skin halves are compressed in the press and bolted together. The compression is done in several steps, while coil stress is monitored by the gauges. Finally, the 50 mm thick end plates are bolted to the skin ends.

Table 3 Coil specific design features.

Mirror	Coil #	Strand	Cable	Cable insulation	Coil poles
TQM01	#19	RRP-54/61	LBNL	S2-glass sleeve	Bronze
TQM02	#17	RRP-54/61	LBNL	S2-glass sleeve	Bronze
TQM03	#34	RRP-108/127	Fermilab	E-glass tape	Titanium

Table 4 Maximum coil pre-stress at room temperature and after cooling dawn.

Mirror model	Coil pre-stress, MPa	
	300 K (measured)	4.5 K (estimated)
TQM01	96	86-96
TQM02	98	88-98
TQM03a	84	74-84
TQM03b	103	123-133

Transverse coil preload and support is provided by stainless steel skin. Axial preload and support is provided through bolts in the end plates. The coil azimuthal stress during assembly and operation is monitored by resistive strain gauges. In the body, resistive strain gauges are glued to the inside surface of the impregnated coil near the pole and next to the midplane. Resistive gauges are also mounted on the inner surface of inner pole blocks. The axial coil preload and longitudinal Lorentz forces are controlled through the resistive gauges installed on the end bolts.

The first two mirror models were assembled with the same coil target prestress of ~100 MPa at room temperature and the final cold peak prestress of ~90 MPa after cooling down. The third mirror (TQM03a) was first assembled and tested with quite low warm and cold prestress of ~80 MPa and then re-assembled to provide the higher coil prestress of ~130 MPa after cooling down. The level of cold prestress was provided by the specific size of vertical shims between the mirror blocks and the upper yoke. The maximum coil prestress at room temperature measured using coil pole gauges and estimated cold coil prestress are reported in Table 4.

Quench origin in the coil during testing is monitored by voltage taps soldered to coil turns in the inner and outer layer, and coil leads. A quench antenna placed between the coil inner surface and the iron mirror blocks independently registers quenches in the coil in the axial direction.

IV. Test Results and Discussion

TQM01, TQM02 and TQM03a-b were tested in liquid He in the Vertical Magnet Test Facility at Fermilab. The standard test plan included magnet training and ramp rate studies at 4.5 and 1.9 K, and temperature dependence measurements. TQM02 was also equipped with midplane strip heaters to study Nb_3Sn coil thermal margin. The results of these studies are reported elsewhere [15].

The results of TQM01-03a/b training and ramp rate dependence measurements at 4.5 and 1.9 K are shown in Figs. 5 and 6.

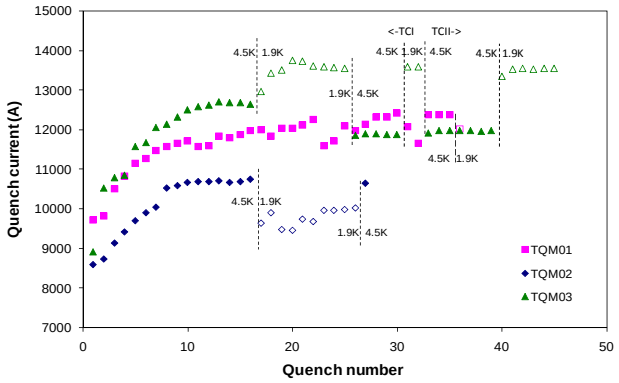

Fig. 5. TQM01-03a/b magnet training at 4.5 and 1.9 K.

The primary goal of TQM01 was to test the mirror design and compare the quench performance of TQ coils in the mirror and quadrupole models TQC02E [10] and TQS02a [16]. All these models used regular TQ coils made of RRP-54/61 Nb_3Sn strand with the only difference that the poles in coil #19 in TQM01 were bronze whereas the coils used in TQC02E and TQS02a had Ti poles. An excellent consistency of coil training in the mirror and quadrupole models was found [17].

During TQM01 training at 4.5 K, a current leak developed between one quench protection heater and ground. During the first quench at 1.9 K a dead short between coil and ground has occurred, resulting in coil damage and discontinuation of the test. Nevertheless, the first quadrupole mirror test confirmed the soundness of the mirror design and its high technical and economical efficiency for single quadrupole coil testing.

The global goal of this mirror series was to study the quench performance of regular LARP TQ coils at 4.5 and 1.9 K including "flux jump" instabilities observed previously in TQ models at 1.9 K [10], and test of a new TQ coil made of the more stable RRP-108/127 strand and modified cable insulation based on E-glass tape at different level of coil prestress.

At 4.5 K all the coils show standard training behavior with some variations of the first quench current, the number of training quenches and the maximum quench current. The ramp rate dependences at 4.5 K for all the coils are also typical.

All quenches near the current plateau in all the coils were located in the outer layer where the field is highest for mirror configuration. This fact, as well as the ramp rate curves, confirms that at 4.5 K the coils reached their conductor limit. The maximum quench current of coil #19 in TQM01 was above 95% of its short sample limit (SSL) calculated using "reference" strand parameters whereas coil #17 in TQM02 reached only 84% of its reference SSL (perhaps due to degradation after multiple re-assembly and tests). Based on witness sample data, coils #19 and #34 reached ~100% of their SSL. Coil #34 made of the new strand and insulation showed the best training performance and highest current.

At 1.9 K the regular TQ coils (#17 and #19) made of RRP-54/61 strand show some reduction of quench current and an erratic quench behavior which is observed also in the ramp rate measurements at the low current ramp rates. One can see as well some unusual increase of the quench current of TQM02 at ramp rates within 200-275 A/s. Meanwhile, coil #34 made of RRP-108/127 strand shows the expected increase of quench current and regular ramp rate dependence at 1.9 K.

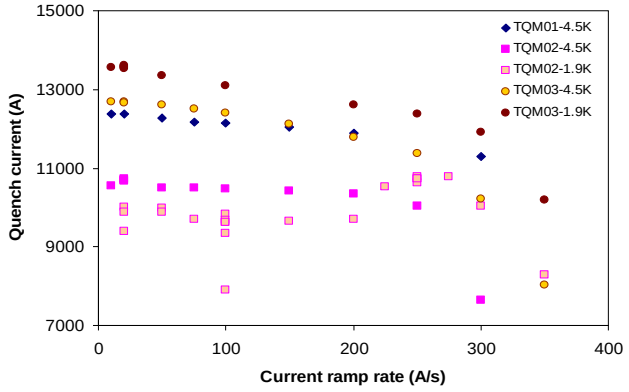

Fig. 6. TQM01-03a/b magnet ramp rate dependences at 4.5 and 1.9 K.

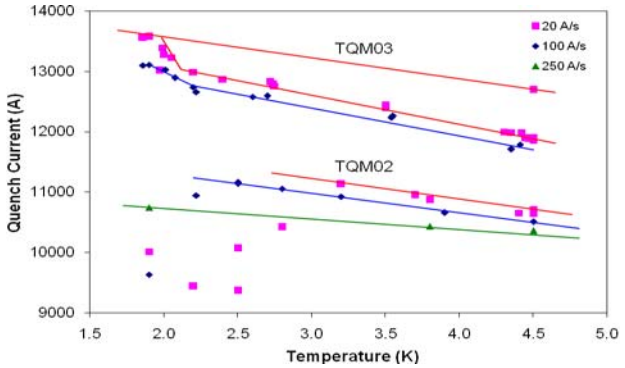

Fig. 7. TQM02 and TQM03a/b quench current vs. helium bath temperatures.

After short training this coil reached 98-99% of its SSL at 1.9 K based on the witness sample data. The training and ramp rate behavior of TQM01 and TQM02 with the regular TQ coils made of RRP-54/61 strand as well as observed improvement of TQM03a quench performance is consistent with the effect of "flux jump" instabilities in Nb_3Sn strands with high Jc and large sub-element size [18].

After quenching at 1.9 K, TQM02 and TQM03a were quenched again at 4.5 K (see Fig.5). While TQM02 confirmed its previously reached maximum quench current, TQM03a demonstrated 6% reduction of the 4.5 K quench plateau. An assumption of possible conductor damage due to the low coil pre-stress in TQM03a and observed coil unloading was not confirmed by the subsequent magnet quenching at 1.9 K. The magnet reproduced its previous quench current plateau at 1.9 K. After re-assembly with higher coil prestress TQM03b demonstrated good training memory at both 4.5 and 1.9 K.

Temperature dependences of magnet quench current were measured in the temperature range of 1.9-4.5 K at different current ramp rates to better understand the flux jump effects in TQM02 and the quench performance observed in TQM03a/b. The results are summarized in Fig. 7. The data for TQM03 near 2.2, 2.3 and 4.5 K were measured in both thermal cycles demonstrating excellent reproducibility of the results.

One can see that TQM02 shows an unstable quench behavior only at temperatures below 2.5-3 K. The transition temperature to the unstable range reduces with the increase of current ramp rate. On the contrary, TQM03 shows stable quench performance at all tested temperatures.

A sharp change of magnet quench current near the lambda-point was observed in TQM03a/b after the first magnet quenching at 1.9 K. This behavior is likely due to the degradation of turn cooling conditions rather than the critical current degradation. This hypothesis will be verified during the coil inspection after magnet disassembly.

V. Conclusion

A quadrupole mirror structure to test single quadrupole coils has been developed and successfully tested. This structure allows testing shell-type coils with the inner radius larger than 45 mm and the outer radius up to 90 mm, including LARP TQ and HQ coils. Two mirror models have been tested with regular LARP 90-mm coils previously used in TQ models. These tests demonstrated high efficiency and consistent coil behavior confirming the soundness of this approach. The coil quench performance in the mirror structure was similar to that of TQ models.

The effect of flux jumps on the quench performance of TQ coils made of Nb_3Sn RRP-54/61 strand at low temperatures has been studied and confirmed. A new TQ coil made of the optimized Nb_3Sn RRP-108/127 strand and new cable insulation was also tested clearly demonstrating improved quench performance and stability at both 1.9 and 4.5 K. The improved stability was also observed during the tests of LARP quadrupole model TQS03 made of the same RRP-108/127 strand [19].

Acknowledgment

The authors thank technical staff of Fermilab's Technical Division for their contributions to magnet fabrication and test.

References

[1] D. R. Chichili, et al., "Design, fabrication and testing of Nb_3Sn shell type coils in mirror magnet configuration," *Adv. Cryogen. Eng.*, Volume 49A, pp. 775–782, 2004.

[2] A.V. Zlobin, et al., "Quench Performance of Nb_3Sn cos-theta coil made of 108/127 RRP Strands," *Adv. Cryogen. Eng.*, Volume 53A, pp. 755–762, 2008.

[3] A.V. Zlobin, et al., "Development of Nb_3Sn accelerator magnet technology at Fermilab," Proceedings of 2007 Particle Accelerator Conference, Albuquerque, NM, June 2007, p.p. 482-484.

[4] G. Chlachidze et al., "Quench performance of a 4-m long Nb_3Sn shell-type dipole coil," *IEEE Trans. on Applied Supercond.*, Volume 19, Issue 3, June 2009 Page(s): 1217 - 1220.

[5] R. Bossert, et al., "Development of TQC01, a 90-mm Nb_3Sn Model Quadrupole for LHC Upgrade Based on SS Collar," *IEEE Trans. on Applied Supercond.*, Volume 16, Issue 2, June 2006 Page(s): 370-373.

[6] S. Feher, et al., "Development and test of LARP technological quadrupole (TQC) magnet," *IEEE Trans. on Applied Supercond.*, Volume 17, Issue 2, June 2007 Page(s):1126-1129.

[7] V.V. Kashikhin, A.V. Zlobin, "Magnetic analysis of LARP TQ mirror models," *Fermilab Technical Division Note*, TD-08-021, June 2008.

[8] S. Caspi et al., "Design of a 120 mm bore 15 T quadrupole for the LHC upgrade phase II," *this conference*.

[9] L.T. Summers, et al., **"**A model for the prediction of Nb_3Sn critical current as a function of field, temperature, strain, and radiation damage," *IEEE Trans. on Magnetics,* Volume 27, Issue 2, March 1991 Page(s): 2041 - 2044.

[10] R. Bossert, et al., "Fabrication and Test of LARP Technological Quadrupole Models of TQC Series," *IEEE Trans. on Applied Supercond.*, Volume 19, Issue 3, June 2009 Page(s): 1226 – 1230.

[11] E. Barzi, et al., "Performance of Nb_3Sn RRP strands and cables based on a 108/127 Stack Design," *IEEE Trans. on Applied Supcond.*, Volume 17, Issue 2, June 2007 Page(s): 2718-2721.

[12] N. Andreev, et al., "Development of Rutherford-type Cables for High Field Accelerator Magnets at Fermilab," *IEEE Trans. on Applied Supercond.*, Volume 17, Issue 2, June 2007 Page(s): 1027-1030.

[13] R. Bossert, et al., "Tests of insulation systems for Nb_3Sn Wind and React Coils," CEC/ICMC'07, Chattanooga, TN, July 16-20 2007.

[14] F. Nobrega et al., "Nb_3Sn Accelerator Magnet Technology Scale-up using Cos-theta Dipole Coils," *IEEE Trans. on Applied Supercond.*, Volume 18, Issue 2, June 2008 Page(s): 273 - 276.

[15] V.V. Kashikhin et al., "Performance of Nb_3Sn quadrupole magnets under localized thermal load," CEC/ICMC'09, Tucson, AR, June 2009.

[16] Caspi, et al., "Test Results of LARP Nb3Sn Quadrupole Magnets Using a Shell-based Support Structure (TQS)," *IEEE Trans. on Applied Supercond.*, Volume 19, Issue 3, June 2009 Page(s): 1221 – 1225.

[17] A.V. Zlobin et al., "Testing of Nb_3Sn quadrupole coils using magnetic mirror structure," CEC/ICMC'09, Tucson, AZ, June 2009.

[18] A.V. Zlobin, V.V. Kashikhin, E. Barzi, "Effect of Magnetic Instabilities in Superconductor on Nb_3Sn Accelerator Magnet Performance," *IEEE Trans. on Applied Supercond.*, Volume 16, Issue 2, June 2006 Page(s): 1308-1311.

[19] H. Felice et al., "Test results of TQS03: a LARP shell-based Nb_3Sn quadrupole using 108/127 conductor," EUCAS2009, August 2009.